Applied Catalysis A: General 358 (2009) 32–41

Contents lists available at ScienceDirect

Applied Catalysis A: General

journal homepage: www.elsevier.com/locate/apcata

Selective liquid-phase hydrogenation of citral over supported bimetallic Pt–Co catalysts

Nicolás M. Bertero [a], Andrés F. Trasarti [a], Bernard Moraweck [b], Armando Borgna [c], Alberto J. Marchi [a,*]

[a] Catalysis Science and Engineering Research Group (GICIC), Instituto de Investigaciones en Catálisis y Petroquímica (INCAPE), FIQ-UNL, CONICET, Santiago del Estero 2654, 3000 Santa Fe, Argentina
[b] Institut de Recherches sur la Catalyse, CNRS, 2 Avenue Albert Einstein, F 69626 Villeurbanne, France
[c] Institute of Chemical and Engineering Sciences (ICES-A*Star), 1 Pesek Road, Jurong Island 627833, Singapore

ARTICLE INFO

Article history:
Received 16 September 2008
Received in revised form 26 January 2009
Accepted 28 January 2009
Available online 6 February 2009

Keywords:
Citral hydrogenation
Aldehydes (α,β-unsaturated)
Platinum-based catalysts
Cobalt-based catalysts
Bimetallic compounds

ABSTRACT

The liquid-phase hydrogenation of citral was studied at 393 K and 10 bar on Pt–Co/C catalysts, having different Pt/(Pt + Co) ratios and containing a total metal load of about 2%. The monometallic and bimetallic Pt–Co/C catalysts were prepared by impregnation and co-impregnation, respectively, with cobalt tris(acetylacetonate) and platinum bis(acetylacetonate). Monometallic Pt/C and Co/C catalysts showed very low activity and selectivity to the desired products. Undesirable reactions, such as citral decarbonylation and hydrogenolysis, were observed with these monometallic catalysts. Instead, bimetallic Pt–Co/C proved very active and selective to geraniol/nerol and the main products detected were geraniol/nerol, citronellal and citronellol. Hydrogenation kinetic constants were determined by modeling catalytic data and using a pseudo-homogeneous kinetics. From the analysis of the kinetic parameters, an optimum Pt/(Pt + Co) ratio was found for both the catalytic activity and selectivity towards geraniol/nerol. Furthermore, it was determined that this optimum ratio depends on the activation conditions. Temperature-programmed reduction (TPR) experiments and X-ray absorption spectroscopy (XAS) demonstrated the existence of Pt–Co bimetallic compounds on the carbon support. On the basis of these results, it was proposed that cobalt improves the catalytic performance of platinum by electron transfer. This electron transfer is favored by the high interaction of both metals existing in these types of bimetallic compounds.

1. Introduction

The selective hydrogenation of unsaturated α,β aldehydes to the corresponding unsaturated alcohols is of considerable interest due to the numerous applications of those alcohols in Fine Chemistry. The selective hydrogenation of citral to geraniol/nerol is of particular importance. These unsaturated alcohols are monoterpenoids that have been employed in the production of flavours, fragrances, insect repellants and in the synthesis of other compounds such as acetate and isobutyrate derivatives [1]. Other products of interest are citronellal and citronellol, used in soaps, detergents, perfumes and insect repellants [1–3]. Citronellal is also important due to its application in topical antifungal compositions for the skin [4]. Besides, it can be hydrated to hydroxycitronellal, which is widely used in fragrances due to its lily-of-the-valley aroma [1]. It can also be isomerized to isopulegol, an intermediary product used in the synthesis of (±)-menthol [5–7]. It can also be used in the production of other compounds employed in fragrances, such as the citronellyl acetate. The geraniol/nerol, citronellal and citronellol mixtures, in adequate proportions, are also employed in fragrances [1], antifungal compositions [8–10], insect repellents [3], bactericide formulations [11] and microbiocidal formulations [12].

The reaction network, considering all the possible hydrogenations starting from citral, is shown in Scheme 1. The geraniol–nerol isomers are obtained by selectively hydrogenating the citral C=O functional group, while citronellal is obtained by the selective hydrogenation of the conjugated C=C bond. In turn, citronellol can be obtained by the selective hydrogenation of the citronellal C=O group or from the C=C bond of geraniol–nerol. The hydrogenation of the isolated C=C bond is not desirable since compounds such as 3,7-dimethyl-octanal and 3,7-dimethyl-octanol give an unpleasant odour to the geraniol–nerol, citronellal and citronellol mixtures.

The selective hydrogenation of citral in liquid phase has been widely studied [13]. In general, catalysts based on noble metals show low activity and/or selectivity in the hydrogenation of unsaturated α,β aldehydes. The activity and selectivity of these

* Corresponding author. Tel.: +54 342 4533858; fax: +54 342 4531068.
E-mail address: amarchi@fiq.unl.edu.ar (A.J. Marchi).

0926-860X/$ – see front matter © 2009 Elsevier B.V. All rights reserved.
doi:10.1016/j.apcata.2009.01.036

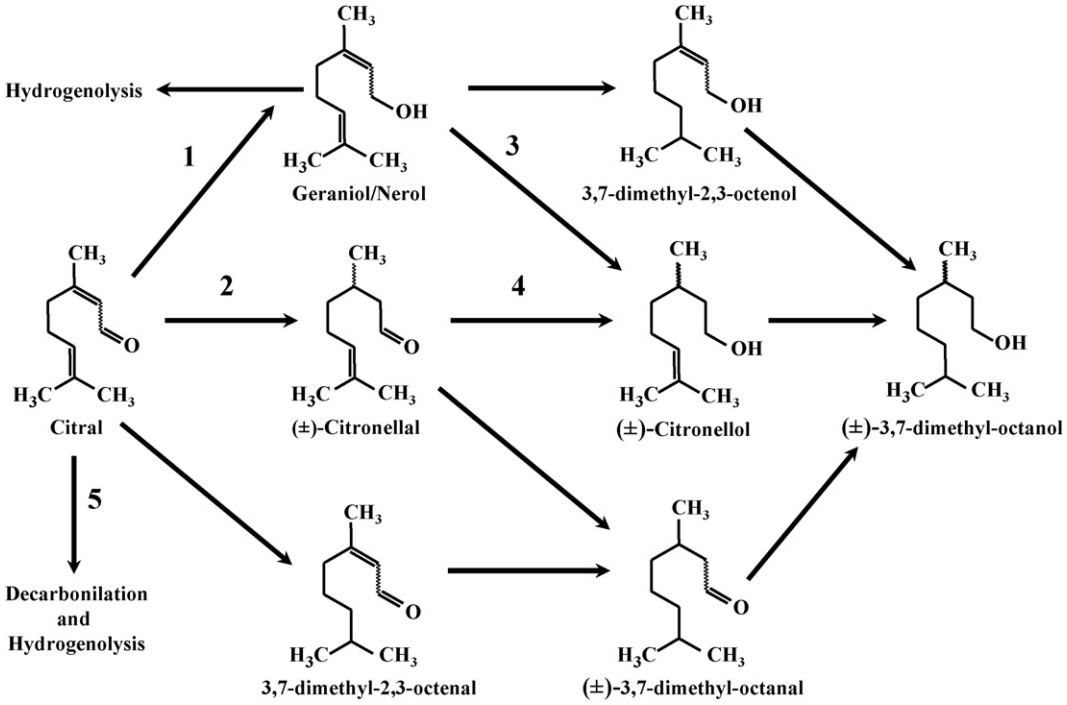

Scheme 1. Reaction network for citral hydrogenation over metal catalysts.

metals can be improved by means of special reduction techniques at low temperature [14–16], interaction of the metallic phase with special supports [17–22] and formation of bimetallic compounds [16,22–33]. In particular, Pt–Co bimetallic catalysts showed a better catalytic performance than those corresponding to Pt monometallic catalysts [16,24,33]. In the liquid-phase hydrogenation of cinnamaldehyde, it was found that Pt–Co catalysts on carbon nanotubes [16] and commercial activated charcoal [24] were more selective to cinnamic alcohol than monometallic catalysts of Pt and Co. Li et al. [16] studied the influence of the preparation method on selectivity, maintaining the Pt/(Pt + Co) ratio. Fouilloux et al. [24] presented the results obtained for different Pt/(Pt + Co) ratios, but he did not account for the high selectivity to cinnamic alcohol observed with Pt–Co bimetallic catalysts. In turn, Borgna et al. [33] studied the hydrogenation of crotonaldehyde at atmospheric pressure over Pt–Co/SiO_2 catalysts, prepared by spin-coating technique. The addition of Co increased the selectivity to crotyl alcohol up to about 25%. From the results obtained by near-edge X-ray adsorption fine structure (NEXAFS), it was proposed that the Pt catalytic performance is modified by the electron transfer from Co. Besides, it is important to bear in mind that the substituting group of the unsaturated α,β aldehyde molecule [34], the type of support, the catalyst preparation method and the reaction conditions [13], can exert a strong influence on the global activity and selectivity in the hydrogenation of this type of compounds.

In this work, we study the catalytic performance of monometallic and bimetallic catalysts of Pt and Co, supported over an activated carbon of high specific surface, in the selective liquid-phase hydrogenation of citral. The goal is to (1) obtain an evidence about the formation of Pt–Co bimetallic compounds; (2) determine the influence that these bimetallic compounds and the Pt/(Pt + Co) ratio have over the hydrogenation of citral in liquid phase. Based on the sample characterization and a pseudo-homogeneous kinetic study, a mechanistic model to explain the experimental results is proposed. This model was built considering both the geometrical and the electronic effect between platinum and cobalt on bimetallic samples.

2. Experimental

2.1. Catalyst preparation

Monometallic Pt/C and Co/C and bimetallic Pt–Co/C catalysts were prepared by wet impregnation and co-impregnation, respectively, employing sub-bituminous carbon of high specific surface (1300 m^2/g) as support. In all the samples, the total metal load in the final catalyst was around 2%. This impregnation was carried out at room temperature for 24 h, using platinum bis(acetylacetonate), $Pt(C_5H_7O_2)_2$, and cobalt tris(acetylacetonate), $Co(C_5H_7O_2)_3$, as impregnating agents. After evaporating the solvent, the precursors obtained were dried under vacuum at 393 K. Finally, the samples were activated *ex situ* in H_2 flow (30 ml/min) at different temperatures between 423 K and 773 K, with no previous calcination, heating them from ambient temperature to reduction temperature at 2 K/min. Samples were kept at the final reduction temperature for 6 h. Mixed oxide elemental compositions were measured by absorption atomic spectrometry (AAS) and the results are shown in Table 1.

2.2. Catalyst characterization

Samples were characterized by temperature-programmed reduction (TPR) and X-ray absorption spectroscopy (XAS).

Temperature-programmed reduction experiments were carried out in a flow system equipped with a quartz microreactor, a temperature controller-programmer and a Balzers GSD 300 mass spectrometer. These experiments were performed with a heating rate of 10 K/min, passing about 30 ml/min of a H_2(5%)/Ar mixture through a dried impregnated sample bed. During programmed heating, *m*/*e* ratios corresponding to the more important fragments of hydrogen, carbon monoxide, carbon dioxide, water, methane, acetaldehyde and propyne were monitored and registered.

XAS measurements were performed at the Lure synchrotron center (ORSAY, France) using a beam line with an energy of 1.85 GeV. All the measurements were performed on the XAFS3

Table 1
Chemical composition of the samples used in this work.

Sample	Metal load[a]		Atomic ratio Pt/(Pt + Co)
	Pt (wt.%)	Co (wt.%)	
Co/C	–	2.10	0
Pt15Co85/C	0.74	1.29	0.148
Pt30Co70/C	1.20	0.83	0.305
Pt50Co50/C	1.59	0.45	0.516
Pt60Co40/C	1.65	0.35	0.636
Pt80Co20/C	1.86	0.17	0.768
Pt/C	1.95	–	1

[a] Determined by atomic absorption spectroscopy.

station in transmission mode using a Si(1 1 1) double-crystal monochromator and two ion chambers. Raw data were recorded by means of a special *in situ* cell equipped with aluminum windows [35], suitable to work from room temperature to 873 K in flowing controlled atmospheres. After reduction at 773 K in flowing H_2, spectra were registered at room temperature at both the Pt–L_{III}-edge (11 564 eV) and Co–K-edge (7709 eV). The EXAFS signal was extracted from raw data by a conventional procedure [36]. A linear background was determined from the lower energy part of the spectrum below the edge and then extrapolated to higher energies. The atomic-like absorption coefficient calculated by a polynomial fit was used as spectrum normalization. The *k*3 weighted EXAFS functions were Fourier transformed (FT).

2.3. Catalytic testing

The liquid-phase hydrogenation of citral (CAL) was studied in a Parr 4843 reactor at 393 K and 10 bar, using isopropanol as solvent. Prior to the catalytic tests, samples were activated *ex situ* in flowing hydrogen (30 ml/min) at different temperatures, between 423 K and 773 K, following the procedure described in Section 2.1. The autoclave was loaded with 150 ml of isopropanol (Aldrich, 98%), 10 ml of citral (Aldrich, 99%) and 1 g of catalyst (particles less than 0.3 mm diameter). The reaction system was heated up to 393 K at 2 K/min and the pressure was then rapidly increased to 10 bar with H_2.

The concentrations of unreacted CAL and of the reaction products were followed during the reaction by *ex situ* gas chromatography using an Agilent 6850 GC chromatograph equipped with flame ionization detector, temperature programmer and a 30-m Innowax (Agilent) capillary column. Samples from the reaction system were taken using a loop under pressure in order to avoid flashing. Data were collected every 15–30 min for 250–500 min, depending on the experiment evolution. Citral conversion (X_{CAL}, mol of citral reacted/mol of citral fed) was calculated as $X_{CAL} = (C^0_{CAL} - C_{CAL})/C^0_{CAL}$, where C^0_{CAL} is the initial concentration of citral and C_{CAL} is the citral concentration at reaction time *t*. It was verified that diffusional restrictions do not corrupt the measurements of the initial reaction rates by carrying out experiments with different catalyst particle sizes and by varying the stirring speed.

3. Results

3.1. Catalyst characterization

Table 1 presents the monometallic and bimetallic samples employed in this work, the metallic load (wt.%) determined by AAS and the molar ratio Pt/(Pt + Co), the latter one obtained from the data of the elemental chemical analysis. In all cases, the Pt and Co contents were varied so as to maintain a total metal load of about 2.0 ± 0.1 wt.%.

3.1.1. Reducibility and decomposition of catalyst precursors

The TPR of the platinum bis(acetylacetonate) sample over sub-bituminous activated carbon (Pt/C) shows an important H_2 uptake around 473 K and a wider but lower H_2 uptake signal approximately at 543 K (Fig. 1). In good agreement with the evolution observed for the H_2 consumption, the signals corresponding to *m*/*e* = 15, 16, 17, 18, 28, 40 and 44 showed two peaks with maxima at 483–493 K and 553–563 K (Fig. 2A). These signals can be attributed to fragments of CH_4, H_2O, CO, C_3H_4 (propyne) and C_2H_4O (acetaldehyde) originated in the decomposition of the platinum bis(acetylacetonate) precursor. The almost coincident evolutions of H_2 consumption and *m*/*e* signals attributed to CH_4, H_2O, CO, C_3H_4 and C_2H_4O indicate that the reduction of Pt^{2+} to Pt^0 is produced almost simultaneously with the acetylacetonate ion decomposition. On this basis, it is proposed that the reductive decomposition of platinum bis(acetylacetonate) over sub-bituminous carbon of high specific surface area, in H_2 atmosphere, takes place mainly through the reaction represented in Scheme 2.

In the case of cobalt tris(acetylacetonate) over sub-bituminous carbon, Co/C sample, the H_2 consumption was registered at higher temperatures than for platinum bis(acetylacetonate). The first H_2 uptake presents a minimum at 580 K. Afterwards, a wide band between 650 K and 750 K was observed (Fig. 1). At the same time, signals corresponding to the *m*/*e* = 15, 16, 28 and 44 fragments were observed, whose maxima are at 593 K and in the 723–753 K range (Fig. 2B). No signals corresponding to *m*/*e* = 17, 18 and 40 were observed. This indicates that H_2O and C_3H_4 are not products of the cobalt tris(acetylacetonate) decomposition in H_2 flow. Besides, between 523 K and 623 K the main signals correspond to *m*/*e* = 15, 16, 28 and 44. These results indicate that in this temperature range, Co^{3+} is reduced to Co^0 simultaneously with the decomposition of the acetylacetonate ion into CH_4, CO and C_2H_4O [reaction (1), Scheme 3]. Instead, at temperatures over 673 K, only the signals corresponding to *m*/*e* = 15, 16 and 28 were observed. It can hence be inferred that in this temperature range cobalt tris(acetylacetonate) is reductively decomposed yielding mainly CH_4 and CO [reaction (2), Scheme 3]. However, in this last case,

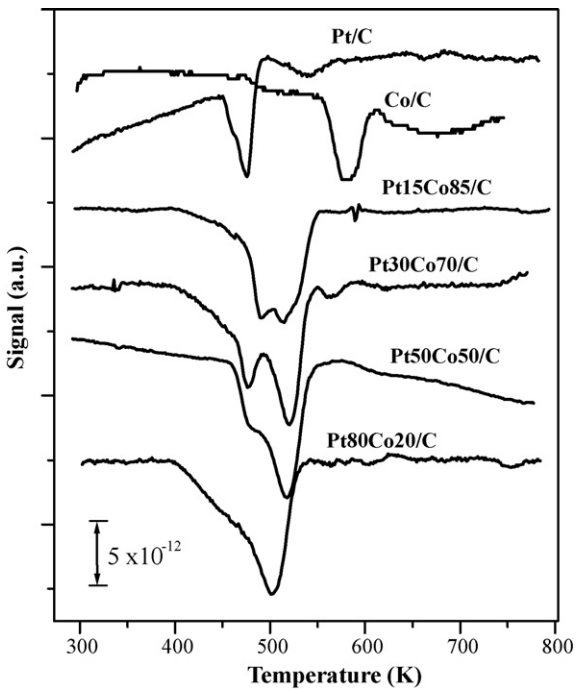

Fig. 1. TPR profiles of monometallic and bimetallic Pt–(Co)/C samples used in the selective hydrogenation of citral in liquid phase.

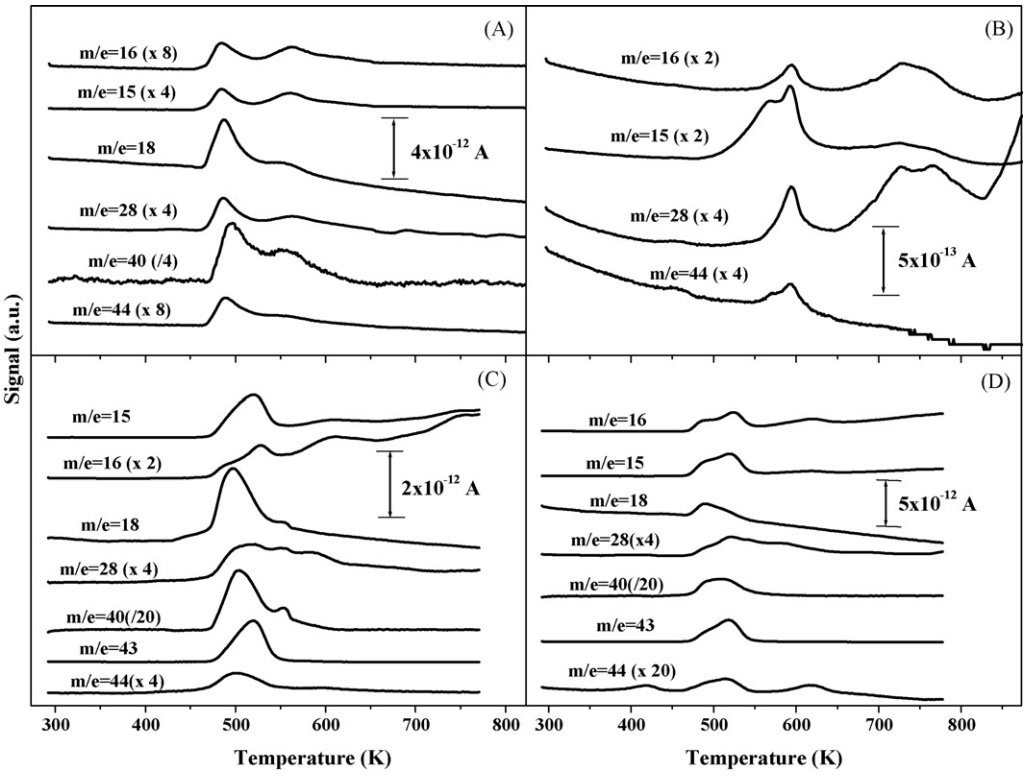

Fig. 2. Evolution of signals detected by MS in the TPR experiments: (A) Pt/C; (B) Co/C; (C) Pt30Co70/C; (D) Pt50Co50/C.

some reductive decomposition of surface functional groups of the support might not be completely disregarded.

For the bimetallic samples Pt15Co85/C and Pt30Co70/C, two overlapped bands of H_2 consumption were observed: one with a minimum between 473 K and 488 K, and the other one with a minimum between 513 K and 523 K. Bimetallic Pt50Co50/C and Pt80Co20/C samples gave a band between 503 K and 513 K with a shoulder between 463 K and 483 K (Fig. 1). In comparison with the profiles obtained for samples Pt/C and Co/C, the first signal was assigned to the platinum bis(acetylacetonate) reductive decomposition. In the same way, the second band was attributed to the reductive decomposition of cobalt tris(acetylacetonate). On the other hand, signals of fragments attributable to both the platinum bis(acetylacetonate) decomposition and cobalt (tris)acetylacetonate (Fig. 2) could be observed. The signals detected were m/e = 15, 16, 18, 28, 40, 43 and 44 in two different temperature ranges: 473–543 K and 573–643 K. The m/e = 43 signal was not observed with the monometallic samples and can be assigned to the C_3H_7 fragment of propane (C_3H_8). The appearance of this signal can be attributed to the fact that part of propyne is likely hydrogenated into propane over the metallic Pt–Co phase formed during the TPR experiment with the bimetallic samples. The shift of 20–30 K, at higher temperatures, observed for the m/e = 43 signal with respect to signals m/e = 40 and 44 is in agreement with this assumption (Fig. 2C and D). Based on the TPRs of the monometallic samples, the other signals in the 473–543 K range can be attributed to the

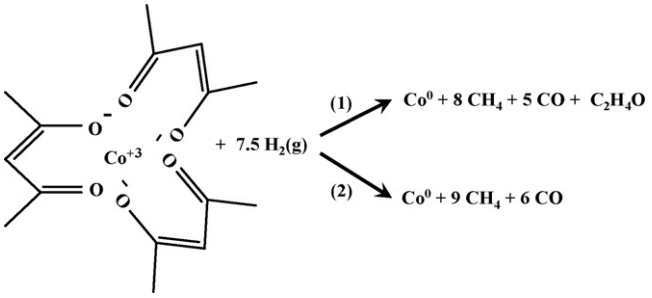

Scheme 3. Reductive decomposition of cobalt tris(acetylacetonate).

simultaneous reductive decomposition of platinum bis(acetylacetonate) and cobalt tris(acetylacetonate) [Schemes 2 and 3 (reaction (1))]. The m/e = 15, 16, 28 and 44 signals observed between 573 K and 643 K can be assigned to the decomposition of the cobalt tris(acetylacetonate) strongly interacting with the surface of the active sub-bituminous carbon. The reductive decomposition of these cobalt tris(acetylacetonate) surface species is catalyzed, as suggested above, by the previously formed Pt^0 phase.

3.1.2. EXAFS

Fig. 3 shows the radial distribution function around Pt for a series of bimetallic Pt–Co/C samples reduced at 773 K. As reference, the Fourier transform corresponding to the monome-

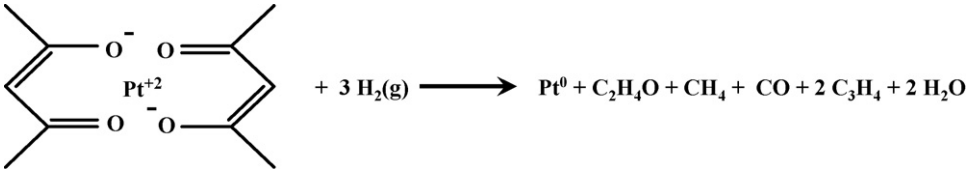

Scheme 2. Reductive decomposition of platinum bis(acetylacetonate).

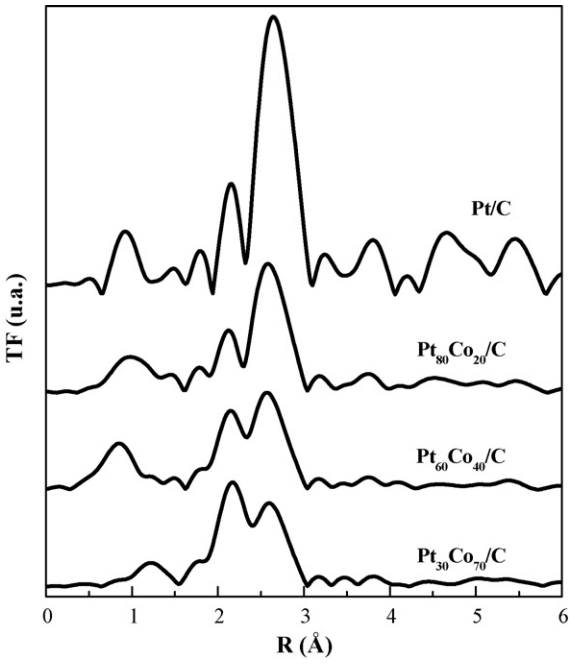

Fig. 3. Fourier transforms of monometallic and bimetallic Pt–(Co)/C samples used in the selective hydrogenation of citral in liquid phase.

tallic Pt/C sample, reduced at the same temperature, is also included. This latter one presents a main peak at 2.62–2.68 Å, corresponding to the Pt–Pt distances and a low-intensity satellite peak at approximately 2.2 Å, which is normally observed for bulk Pt when the FT has not been corrected for the amplitude and phase shift of Pt [38].

As the Co content increases, the intensity of the peak at 2.62–2.68 Å decreases. At the same time, the relative intensity of the peak at 2.2 Å significantly increases with respect to the peak at 2.62–2.68 Å. Indeed, it can be observed that for the samples with more Co content, the intensity of the peak at 2.2 Å is similar to or even greater than that of the peak at 2.62–2.68 Å. These results clearly show that after the treatment in H_2 at 773 K, the local environment of Pt in the bimetallic samples is significantly different from that of the monometallic Pt/C sample.

Fig. 4A and B shows the XANES spectra at the L_{III}-edge of Pt and K-edge of Co, respectively. While no significant differences are observed at the L_{III}-edge of Pt (Fig. 4A) on the monometallic Pt/C sample as compared to the Pt foil spectrum, the XANES spectra of the Pt–Co bimetallic samples are significantly modified, exhibiting a substantial decrease of the white line. The $L_{2,3}$-edges of 5d metals have been frequently used to study electronic modifications of the d-band in catalysis research, attributing an increase or decrease of the intensity of the white line to an electronic modification of the absorbing atoms [39,40]. A decrease of the white line can be associated with a decrease of the number of d-holes in the Pt 5d band. Fig. 4B shows that the Co–K-edge of the bimetallic samples is also significantly modified. As compared to the Co foil, Pt–Co samples exhibit a decrease of the 1s → 3d transitions while the transitions 1s → 4s, 4p are increased, suggesting a decrease of the electronic density of Co. In summary, XAS is clearly showing that the Pt environment and its electronic properties are strongly modified by the presence of Co.

3.2. Catalytic tests

3.2.1. Citral hydrogenation

The monometallic samples, after reduction in hydrogen flow at 773 K, showed low activity in the liquid-phase citral hydrogenation at 393 K and 10 bar. However, the bimetallic samples, reduced under the same conditions, were much more active than the monometallic ones (Fig. 5A). Catalytic tests using sub-bituminous carbon, without metal, showed negligible activity under similar reaction conditions. These results are indicating that (1) metal phase is necessary for citral conversion; (2) the hydrogenating capacity of the bimetallic samples is higher than the corresponding to the monometallic samples. This is in agreement with the differences observed between the monometallic and bimetallic samples in the TPR experiments. Besides, for a given reaction time, the conversion of citral increases from Co/C up to Pt30Co70/C. Afterwards, for Pt/(Pt + Co) ratios higher than 0.3, the citral conversion decreases up to Pt/(Pt + Co) = 1, i.e., the Pt/C sample.

It was also determined that the main reaction products were geraniol, nerol, citronellal and citronellol. As an example, Fig. 5B presents the product distribution as a function of time for the case of the bimetallic Pt30Co70/C sample. For the monometallic samples and some bimetallic ones, particularly in the case of Co/C, other products were detected, presumably derived from citral and geraniol/nerol hydrogenolysis and/or decarbonylation.

As can be observed in Scheme 1, the reaction system can be extremely complex, depending on the catalyst type and the

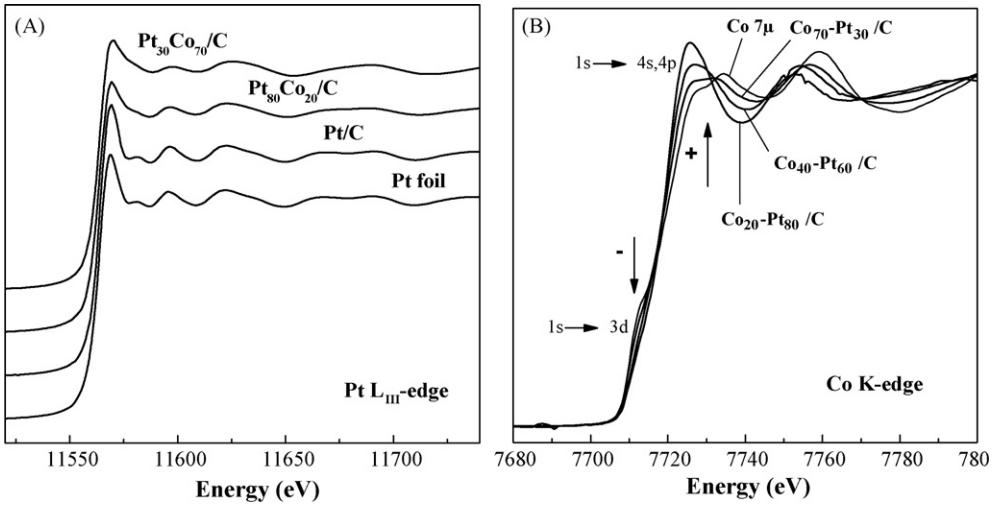

Fig. 4. (A) Normalized Pt–L_{III}-edge XANES spectrum of reduced Pt–Co/C bimetallic catalysts as compared to those of reduced Pt/C catalyst and Pt foil. (B) Normalized Co–K-edge XANES spectrum of reduced Pt–Co/C bimetallic catalysts as compared to that of Co foil.

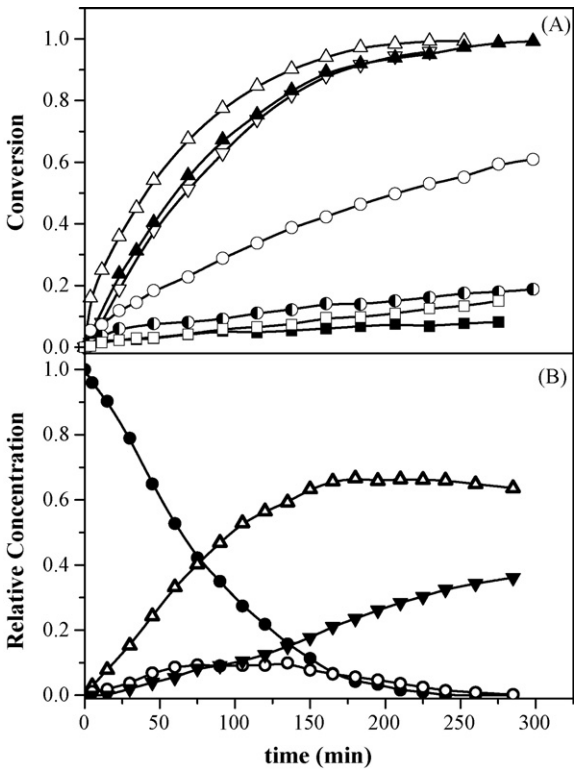

Fig. 5. Liquid-phase citral (CAL) hydrogenation with monometallic and bimetallic Pt–(Co)/C catalysts. T = 393 K; P = 10 bar; W_{cat} = 1 g; V_{CAL} = 10 ml; V_{SOLV} = 150 ml. (A) Citral conversion. (■) Pt/C; (□) Co/C; (▲) Pt15Co85/C; (△) Pt30Co70/C; (▽) Pt50Co50/C; (○) Pt60Co40/C; (◐) Pt80Co20/C. (B) Evolution with time of product and reactant concentrations for Pt30Co70/C catalyst. (●) Citral; (△) geraniol/nerol; (○) citronellal; (▼) citronellol.

reaction conditions employed. The bimetallic Pt–Co/C catalysts employed in this work were highly selective in the hydrogenation of the functional group C=O and the conjugated bond C=C (stages 1–4, Scheme 1). In no case products derived from the hydrogenation of the isolated C=C bond of citral or from undesirable by-reactions, such as hydrogenolysis or decarbonylation, were observed. Instead, monometallic catalysts showed activity in the hydrogenolysis and/or decarbonylation of citral and in the hydrogenolysis of unsaturated alcohol. The activity of these monometallic catalysts in the hydrogenation of the isolated C=C bond was either very low or null. Initially, Pt–Co/C catalysts hydrogenate citral in order to yield (±)-citronellal and geraniol–nerol isomers as main products. After reaching a maximum, the concentration of citronellal and geraniol–nerol in the mixture decreases with reaction time (Fig. 5B). Thus, considering the induction period observed, (±)-citronellol is obtained by the hydrogenation of citronellal and geraniol–nerol. At the same time, the results obtained indicate that the highest concentration of geraniol–nerol in the liquid phase is reached with the bimetallic Pt30Co70/C catalyst. These results show that (1) the bimetallic Pt–Co/C catalysts are much more active and selective to geraniol–nerol than monometallic Pt/C and Co/C in the hydrogenation of citral; (2) the activity and selectivity depend on the Pt/(Pt + Co) ratio.

Summing up, the most remarkable facts observed in the catalytic activity experiments performed in this work are the following: (1) monometallic Pt/C and Co/C catalysts showed low activity in the hydrogenation of citral in liquid phase; (2) an important activity for this reaction can only be obtained with the bimetallic Pt–Co/C catalysts; (3) the highest activity and selectivity to geraniol–nerol seems to be obtained with the bimetallic Pt30Co70/C catalyst; (4) the bimetallic Pt–Co/C catalysts were less active than the monometallic ones in the hydrogenolysis and decarbonylation reactions; (5) no induction period is observed in the formation of decarbonylation and/or hydrogenolysis products, which suggests that most of them are obtained from citral.

In order to confirm these observations, a kinetic study was carried out employing a first-order pseudohomogeneous model. The results of this kinetic study are detailed and discussed below.

3.2.2. Kinetic analysis

In order to determine the hydrogenation kinetic constant values we performed a kinetic study by fitting catalytic data using a first-order pseudohomogeneous model. In accordance with the results described above, the reaction network shown in Scheme 1 may be reduced to reactions (1)–(5) when Pt–(Co)/C catalysts are used. Thus, the kinetics of citral (CAL) hydrogenation is represented by the following differential equations system, i.e., Eqs. (1)–(5), which includes the CAL conversion rate and the formation rates of geraniol/nerol (GOL), citronellal (CNAL), citronellol (CNOL) and products of citral decarbonylation and hydrogenolysis (DH):

$$r_{CAL} = -\frac{dC_{CAL}}{dt} = k_1 C_{CAL} + k_2 C_{CAL} + k_5 C_{DH} \quad (1)$$

$$r_{GOL} = \frac{dC_{GOL}}{dt} = k_1 C_{CAL} - k_3 C_{GOL} \quad (2)$$

$$r_{CNAL} = \frac{dC_{CNAL}}{dt} = k_2 C_{CAL} - k_4 C_{CNAL} \quad (3)$$

$$r_{CNOL} = \frac{dC_{CNOL}}{dt} = k_3 C_{GOL} + k_4 C_{CNAL} \quad (4)$$

$$r_{DH} = \frac{dC_{DH}}{dt} = k_5 C_{CAL} \quad (5)$$

The differential equation system (1)–(5) was solved numerically using the Runge–Kutta–Merson algorithm. The model parameter estimation was performed by non-linear regression using a Levenberg–Marquardt algorithm which minimizes the following objective function: $Q = \sum (C_{i,j} - C^*_{i,j})^2$, where C and C^* are the experimental and calculated concentrations, respectively, i the chemical compound, and j is the reaction time. In all the cases the kinetic parameters were statistically significant (different from zero) with a 95% confidence.

By applying the first-order pseudohomogeneous model represented by Eqs. (1)–(5) it was possible to estimate the kinetic constants and initial hydrogenation rates of citral to geraniol–nerol (k_1, r_1^0), to citronellal (k_2, r_2^0) and to the primary products of decarbonylation/hydrogenolysis (k_5, r_5^0). Fig. 6 shows the initial rates of reaction as a function of the relative atomic percent of Pt with respect to Co, for two activation temperatures: 548 K (Fig. 6A) and 773 K (Fig. 6B). For the samples reduced at either 548 K or 773 K, the hydrogenation rate to both geraniol–nerol and citronellal presents a maximum for a given Pt/(Pt + Co) ratio. Instead, r_5^0 goes through a minimum when the activation temperature is 773 K. The Pt/(Pt + Co) ratio for which the maximum reaction rate to geraniol/nerol and citronellal is obtained depends on the temperature used during the activation process in H_2 flow. When the reduction temperature was 548 K, the maximum activity was obtained with the bimetallic Pt15Co85/C catalysts (Fig. 6A). Instead, when the H_2 activation was performed at 773 K, the maximum activity was observed for the bimetallic Pt30Co70/C catalyst (Fig. 6B).

The increase of the initial hydrogenation rate to geraniol–nerol with the bimetallic Pt30Co70/C sample compared to the monometallic Pt/C sample was up to 4–5 times higher than the increase observed for the initial hydrogenation rate to citronellal (Fig. 6). Instead, the highest initial rates of hydrogenolysis and decarbo-

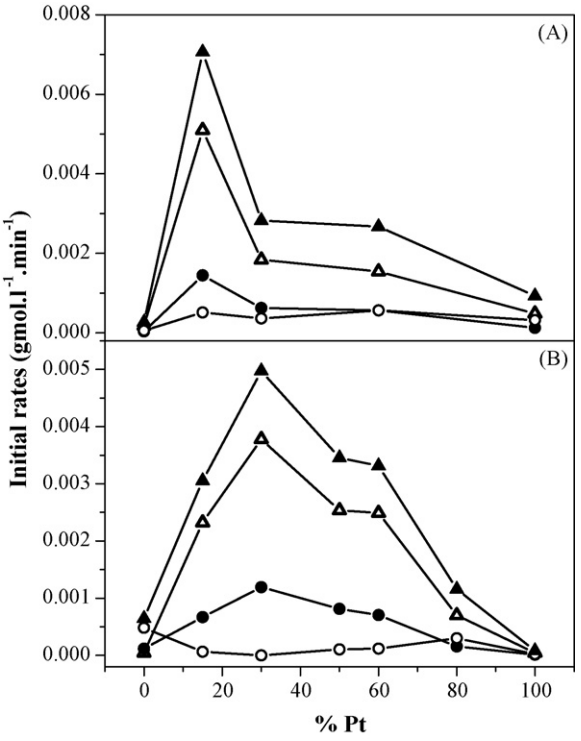

Fig. 6. Initial reaction rates calculated from pseudohomogeneous model (reaction order one with respect to citral, citronellal and geraniol–nerol). Catalyst activation at (A) 548 K and (B) 773 K. (▲) Global initial reaction rate; (△) initial reaction rate to geraniol/nerol; (●) initial reaction rate to citronellal; (○) initial reaction rate to others.

nylation were obtained for the monometallic Pt/C and Co/C samples, activated at 548 K and 773 K, respectively. Moreover, these decarbonylation and hydrogenolysis reactions are practically inhibited in the bimetallic Pt–Co samples, activated in H_2 at 773 K. In general, for the bimetallic samples, the initial rate of citral decarbonylation and/or hydrogenolysis was one to two orders of magnitude lower than the initial hydrogenation rates to citronellal and to geraniol–nerol.

Fig. 7 presents the selectivity to geraniol–nerol, defined as $k_1/(k_1 + k_2 + k_5)$, as a function of the Pt atomic percent for the two activation temperatures. It can be observed that the selectivity to geraniol–nerol reaches a maximum with the Pt/(Pt + Co) ratio. When the activation of the samples is performed at 548 K, the maximum selectivity to the unsaturated alcohols, geraniol/nerol, is again obtained for Pt15Co85/C. Instead, for the samples reduced at 773 K, this maximum is obtained from Pt/(Pt + Co) = 0.15 to Pt/(Pt + Co) = 0.6. In brief, it is confirmed that the bimetallic samples of Pt–Co are not only much more active than the corresponding monometallic Pt and Co samples but also more selective to the unsaturated alcohol geraniol/nerol.

In order to get additional information about the influence of a bimetallic Pt–Co phase on activity and selectivity in citral hydrogenation, the results obtained with some selected samples activated at three different reduction temperatures were analyzed. The initial reaction rates and the selectivities to geraniol–nerol as a function of the activation temperature are shown in Fig. 8A and B, respectively. For Pt/C it was observed that the conversion rate of citral to geraniol–nerol, citronellal and by-products decreases dramatically with the increase of the activation temperature (Fig. 8A), whereas the selectivity to geraniol–nerol varies slightly (Fig. 8B). Instead, in Co/C it could be observed that the global citral conversion rate increases with the activation temperature. However, the relative increase of the reaction rate with the

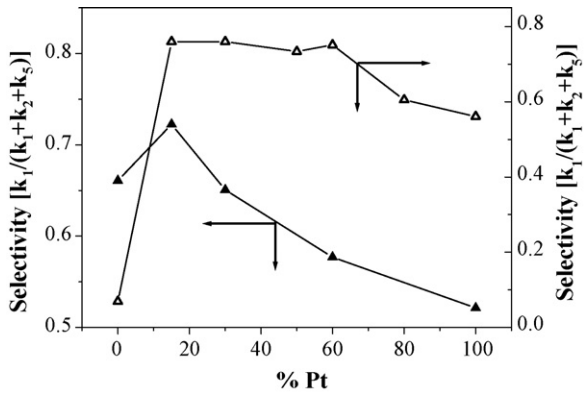

Fig. 7. Selectivity to geraniol/nerol, defined as $k_1/(k_1 + k_2 + k_5)$, in the liquid-phase citral hydrogenation with monometallic and bimetallic Pt–(Co)/C catalysts. Catalyst activation at 548 K (▲) and 773 K (△).

activation temperature was much more important for the by-reactions than for the hydrogenation to citronellal and geraniol–nerol (Fig. 8A). This is causing an important drop of the selectivity to geraniol–nerol (Fig. 8B). A completely different behavior was found for the bimetallic Pt30Co70/C catalyst. In this case, the hydrogenation reactions to geraniol–nerol and citronellal increased with the activation temperature, while the rate of formation of by-products markedly decreased (Fig. 8A). Then, we can affirm that for the Pt30Co70/C sample an increase of both total activity and selectivity to geraniol–nerol with the activation temperature was obtained. These results confirm that the bimetallic Pt–Co phase has a catalytic behavior completely different from that observed for the monometallic phases formed in Pt/C and Co/C samples.

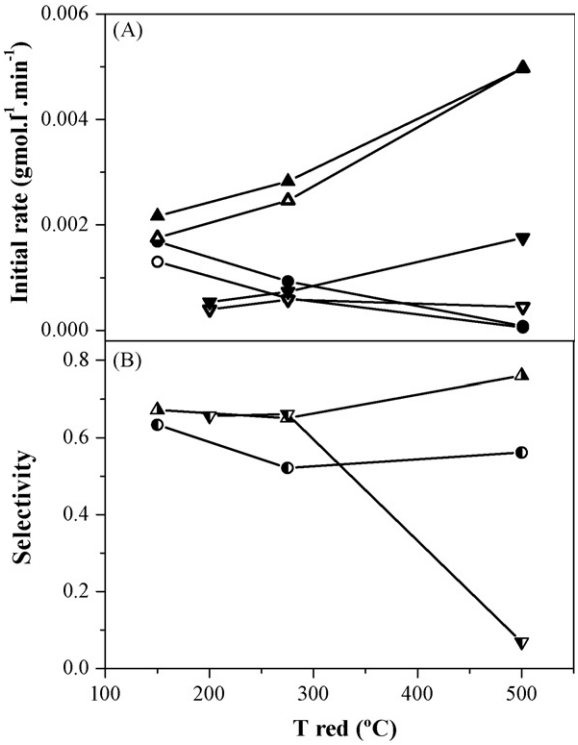

Fig. 8. Initial reaction rates and selectivities to geraniol/nerol varying the activation temperature. (A) Initial rates. (▲, △) Pt30Co70/C; (●, ○) Pt/C; (▼, ▽) Co/C. Full symbols: initial global rates; open symbols: initial hydrogenation rates. (B) Selectivities to geraniol/nerol defined as $k_1/(k_1 + k_2 + k_5)$. (◭) Pt30Co70/C; (◐) Pt/C; (◬) Co/C.

4. Discussion

The results obtained in the catalytic tests show that the functional C=O group and the conjugated C=C bond of citral are selectively hydrogenated over the bimetallic Pt–Co/C catalysts employed in this work. In no case hydrogenation of the citral isolated C=C bond was observed. Besides, other undesirable reactions such as decarbonylation and hydrogenolysis, which do occur with monometallic Pt/C and Co/C catalysts, are inhibited on these bimetallic Pt–Co/C catalysts, especially when they are activated at 773 K. Finally, it was determined that there is an optimum Pt/(Pt + Co) ratio for the citral hydrogenation rate and for the selectivity to the geraniol–nerol isomers. This optimum composition varies with the activation conditions.

The physicochemical characterization of the Pt–Co/C catalysts by RTP and XAS allowed us to obtain evidence about the formation of a bimetallic Pt–Co compound on the surface of the sub-bituminous carbon of high specific surface employed as support.

The TPR profile of the monometallic Pt/C sample shows bands of H_2 consumption (Fig. 1) and signals of fragments produced by the reductive decomposition of the acetylacetonate ion (Fig. 2) at temperatures considerably lower than those observed for the monometallic Co/C sample. These results are clearly indicating that, in H_2 flow, platinum bis(acetylacetonate) is considerably less stable than cobalt tris(acetylacetonate). Instead, the reductive decomposition of platinum bis(acetylacetonate) and cobalt tris(acetylacetonate) in the bimetallic Pt–Co/C samples occurs almost simultaneously. This overlapping is due to the fact that while the main H_2 consumption band of platinum bis(acetylacetonate) occurs always practically at the same temperature, that of cobalt tris(acetylacetonate) shifts 50–70 K to lower temperatures. This shift can be attributed to catalytic effect of hydrogen dissociatively chemisorbed on Pt^0, which was formed by previous reduction of platinum bis(acetylacetonate). Consequently, the cobalt tris(acetylacetonate) reduction is produced at lower temperatures than in the monometallic Co/C sample [37]. The simultaneous reductive decomposition of platinum bis(acetylacetonate) and cobalt tris(acetylacetonate) increases the probability of forming bimetallic Pt–Co particles, even at relatively low temperatures [41]. The formation of these bimetallic compounds would result in a more active metallic phase than the one obtained with the monometallic samples. Then, this would explain the hydrogenation of propyne into propane observed in the TPRs of the bimetallic Pt–Co/C samples (Fig. 2C and D), which was not detected with the monometallic samples (Fig. 2A and B).

The EXAFS spectra show that the relative intensity of the satellite peak at 2.2 Å with respect to the peak at 2.62–2.68 Å increases with the Co content, is giving evidence of an alteration of the Pt atoms environment in the bimetallic Pt–Co/C samples. In a previous work [42], we have demonstrated that the existence of a short-distance peak indicates the existence of Pt–M bimetallic interactions. Furthermore, the decrease of the white line observed on the XANES spectra for the Pt–Co bimetallic samples indicates an increase of the electronic density of Pt, probably via electron transfer or rehybridization of the orbitals upon alloying. Similarly, other authors [43,44] also reported an electronic transfer from nickel and iron to platinum. In a previous work, Borgna et al. [33] using *in situ* NEXAFS on model bimetallic Pt–Co/SiO_2 catalysts prepared by spin-coating techniques, demonstrated that there is an increase in the density of (DOS) d states of cobalt. This is probably due to an electronic transfer or rehybridization of these orbitals. Based on these results, it is proposed that Pt and Co form bimetallic particles in which the cobalt electronic density decreases due to the electron transfer towards platinum. The fractional charge transfer increases with the Pt/(Pt + Co) ratio. As a consequence of this modification in the electronic density of platinum and cobalt, an important modification of the catalytic and adsorptive properties of these metals would be expected.

In sum, our results obtained by XAS clearly show that the Pt environment and its electronic properties are strongly modified by the presence of Co, revealing the existence of alloyed Pt–Co. This is in good agreement with previously discussed TPR results, which also suggest the formation of bimetallic Pt–Co particles.

The formation of these bimetallic compounds could explain the greater activity and selectivity observed with the Pt–Co/C samples with respect to the monometallic Pt/C and Co/C ones. Based on the TPR and XAS results, it is assumed that on the surface of Pt–Co/C catalysts there are clusters formed by both Pt^0 and Co^0 atoms in intimate contact. This contact between both types of atoms favors the electronic transfer from Co^0 towards Pt^0, as determined by XAS. In this way, there is $+\delta$ charge density in the Co atoms and a $-\delta$ charge density in the Pt atoms (Scheme 4). On the other hand, considering a molecule of unsaturated α,β aldehyde, it is accepted that the functional C=O group could be adsorbed on-top, di-σ_{CO} and π_{CO} over a metal surface [34]. Similarly, for the C=C group, the most likely adsorption modes are di-σ_{CC} and π_{CC}. According to the

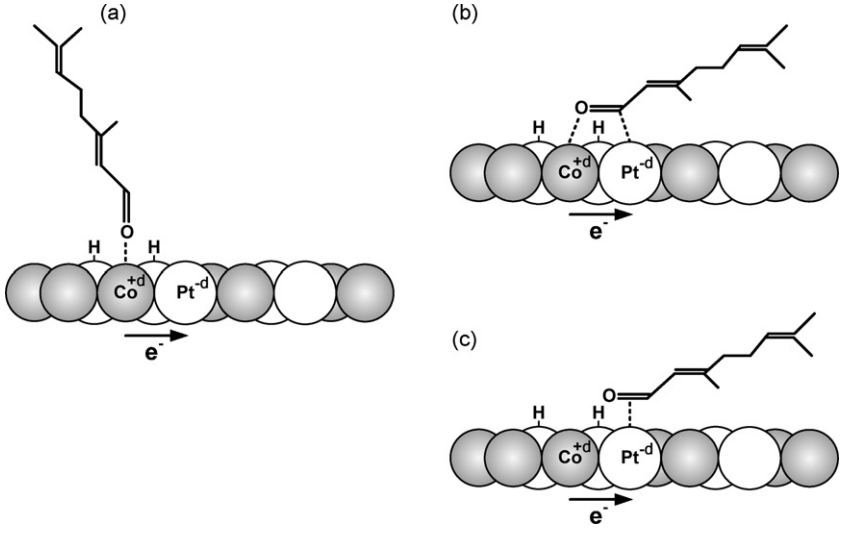

Scheme 4. Citral adsorption modes over Pt–Co/C catalysts: (a) on-top; (b) di-σ_{CO}; (c) π_{CO}.

analysis performed by Delbecq and Sautet [34], taking into account the interaction of different unsaturated α,β aldehydes with Pt, as an average, the bonding energy follows the pattern: di-$\sigma_{CO} \cong \pi_{CO}$ > on-top. On the other hand, the bonding energies calculated for di-σ_{CC} and π_{CC} are comparable to those of di-σ_{CO} and π_{CO}. Based on this analysis, it is expected that, in the citral hydrogenation, geraniol/nerol and citronellal would be obtained in similar amounts over Pt^0 clusters. Results reported by other authors for the citral hydrogenation in liquid phase with Pt-based catalysts are in agreement with this analysis [6,7]. However, on a bimetallic Pt–Co surface, it is likely that the following interactions are the most favored: (a) on-top adsorption over $Co^{\delta+}$ (Scheme 4a); (b) di-σ_{CO} adsorption over $Pt^{\delta-}$–$Co^{\delta+}$ (Scheme 4b); (c) π_{CO} adsorption over $Pt^{\delta-}$ (Scheme 4c). The on-top adsorption over $Co^{\delta+}$ is more probable than over Pt^0 of monometallic Pt/C sample. This is due to the fact that the electrophilic character of Co in the bimetallic Pt–Co compound is much higher than that of Pt^0 in monometallic Pt/C. As a consequence, the interaction of an electron pair of the oxygen in the C=O group with a $Co^{\delta+}$ site is much more likely than with Pt^0. The di-σ_{CO} adsorption would occur by the interaction between the O atom and $Co^{\delta+}$ and between the C atom and $Pt^{\delta-}$ (Scheme 4b). The $C^{\delta+}$–$O^{\delta-}$ charge separation, enhanced after the interaction with the active site, is favoring the di-σ_{CO} adsorption over a $Pt^{\delta-}$–$Co^{\delta+}$ site against a Pt–Pt site. Likewise, the π_{CO} adsorption over $Pt^{\delta-}$ would be favored with respect to Pt^0. This may be explained by the back-bonding from the platinum orbitals with increased electronic density in the bimetallic samples towards the π^* molecular orbital of C=O group. This would further weaken the C=O bond adsorbed in π_{CO} mode activating it for its subsequent hydrogenation to C–OH. In all cases, the hydrogen dissociatively adsorbed in neighbouring Pt atoms would allow the easy hydrogenation of the functional C=O group adsorbed in one of the three proposed modes (Scheme 4), all of which are more active than the C=O group adsorbed on a Pt^0 cluster.

In turn, when the citral is adsorbed through the C=O group over the bimetallic Pt–Co surface, the interaction with the C=C bond would be decreased by the repulsion effect between the citral substituting group and the Pt–Co surface (Scheme 4). The ratio of the repulsion forces with respect to the attraction forces, between the citral substituting group and the metallic surface, is increasing by (1) the higher electronic density of Pt orbitals in the bimetallic samples with respect to monometallic Pt/C; (2) the extension of the d orbitals of Co. However, the interaction between the C=C bond and the Pt atoms is still possible through the π_{CC} adsorption mode. This adsorption mode, similar to what occurs with the π_{CO} mode, would be favored over $Pt^{\delta-}$ with respect to Pt^0, explaining the higher hydrogenation rate of citral to citronellal over Pt–Co/C than over Pt/C and Co/C. However, on the basis of the results obtained in this work, the increase in the activation of the conjugated C=C bond is less important than the activation increase of the C=O group by adsorption through modes on-top, di-σ_{CO} and π_{CO} over Pt–Co.

In sum, the probability of interaction and activation of the functional C=O group and, to a lesser extent, of the C=C bond with the catalytic surface is expected to be higher with the bimetallic Pt–Co/C catalysts than with the monometallic Pt/C and Co/C samples. This would explain the higher activity of the former in the citral hydrogenation in liquid phase. On the other hand, the higher probability of interaction and activation of the functional C=O group with respect to the C=C bond would also explain the high selectivity to geraniol/nerol observed with these bimetallic catalysts.

Additional evidence of the formation of these bimetallic compounds was obtained in catalytic tests with monometallic Pt/C and Co/C catalysts and with the bimetallic Pt30Co70/C catalyst reduced at different temperatures. In the case of the monometallic samples, the drop observed for the global hydrogenation rate can be explained by the sintering of the corresponding metallic phase with the increasing activation temperature. Instead, the increase of the reaction rate observed with the bimetallic Pt30Co70/C sample can be attributed to the greater formation of bimetallic compound in optimum proportions.

Both the citral hydrogenation rate and the selectivity to unsaturated alcohols go through a maximum for a given Pt/(Pt + Co) ratio. It was determined that this maximum depends on the activation conditions carried out prior to the catalytic activity tests. For example, when the reduction temperature was 548 K, the optimum was obtained for the case of Pt15Co85/C. Instead, when the activation temperature was 773 K, the optimum was found for Pt30Co70/C. This could be related with the fact that the surface bimetallic Pt–Co compound of optimum composition could be more easily obtained at low temperatures for a Pt/(Pt + Co) = 0.15 ratio, in agreement with that observed in the TPR experiments. However, with the temperature increase, the existence of surface enrichment in cobalt is possible, giving place to a higher dilution of the platinum phase and, consequently, to a less active phase [41,45]. On the contrary, when the bulk ratio is Pt/(Pt + Co) = 0.3, the formation of the surface active phase of the optimum composition is obtained at higher temperatures. In this way, the dilution effect at 773 K is smaller in Pt30Co70/C than in Pt15Co85/C and, therefore, the activity maximum is observed for Pt/(Pt + Co) = 0.3.

5. Conclusions

The bimetallic Pt–Co samples supported over sub-bituminous activated carbon, of high specific surface, are much more active and selective in the citral hydrogenation to geraniol/nerol than the monometallic Pt/C and Co/C catalysts. The undesired reactions, such as decarbonylation and hydrogenolysis, observed with Pt/C and Co/C can be inhibited with the bimetallic Pt–Co/C catalysts activated at 773 K in H_2 flow. In addition, we determined that, depending on the activation temperature, there is an optimum Pt/(Pt + Co) ratio through which the highest hydrogenation rate of citral to geraniol–nerol and citronellal is reached.

The behavior of the Pt–Co/C samples can be explained by the formation of bimetallic Pt–Co compounds on the surface of the support, a sub-bituminous carbon. The formation of bimetallic Pt–Co clusters would be favored by (1) the quasi-simultaneous reductive decomposition of the platinum and cobalt precursors; (2) the high initial interaction of the platinum and cobalt precursors over the support surface, favored by the preparation method employed. This high interaction between platinum and cobalt is retained in the final catalysts, allowing electron transfer from cobalt to platinum. Both the intimate Pt–Co contact and the electronic transfer favor the citral adsorption over Pt–Co/C, with respect to Pt/C and Co/C, both through the C=O group and the C=C bond. The citral adsorption modes through the C=O group, namely (a) on-top, by the interaction of the citral oxygen atom with $Co^{\delta+}$; (b) di-σ_{CO}, by the interaction of the oxygen atom with $Co^{\delta+}$ sites and carbon atom with $Pt^{\delta-}$; (c) π_{CO}, by the interaction of the C=O group with $Pt^{\delta-}$, are all favored if compared to the equivalent modes over Pt^0 clusters. For the citral adsorption through the C=C group, the most feasible adsorption mode is π_{CC}. This interaction is diminished because of the repulsion forces between substituting group of citral and the metal surface. In this way, the interaction of the Pt–Co/C active surface with C=O is more effective than with the citral conjugated C=C bond. Consequently, the citral hydrogenation to geraniol/nerol over Pt–Co/C is favored against the hydrogenation to citronellal, different from what happens over Pt-based catalysts.

Acknowledgements

We thank the Universidad Nacional del Litoral (UNL), Consejo Nacional de Investigaciones Científicas y Técnicas (CONICET) and Agencia Nacional de Promoción Científica y Tecnológica (ANPCyT), Argentina, for the financial support of this work. Finally, we would like to thank Prof. Elsa Grimaldi for editing the English of the paper.

References

[1] Kirk-Othmer Encyclopedia of Chemical Technology, 4th edition.
[2] W.G. Taylor, C.E. Schreck, J. Pharm. Sci. 74 (5) (1985) 534.
[3] J.-K. Kim, C.-S. Kang, J.-K. Lee, Y.-R. Kim, H.-Y. Han, H.K. Yun, Entomol. Res. 35 (2) (2005) 117.
[4] R.G. Farinas, US Patent 5,486,537 (1996) to Dayton Laboratories, Inc.
[5] Y. Nakatani, K. Kawashima, Synthesis 2 (1978) 149.
[6] A.F. Trasarti, A.J. Marchi, C.R. Apesteguía, J. Catal. 224 (2004) 484.
[7] A.F. Trasarti, A.J. Marchi, C.R. Apesteguía, J. Catal. 247 (2007) 155.
[8] S. Pattnaik, V.R. Subramanyam, C. Kole, Microbios 86 (349) (2006) 237.
[9] M. Hanada, H. Iwai, J. Fujigasaki, US Patent 6,960,350 (2005) to Takasago Int. Corporation.
[10] M. Hanada, H. Iwai, J. Fujigasaki, US Patent Application 2002/0177621 A1.
[11] H. Yamada, H. Ishida, K. Tkukuda, US Patent Application 2004/0132630 A1.
[12] S. Ben-Yehoshua, US Patent Application 2004/0234662 A1.
[13] H.O. Gallezot, D. Richard, Catal. Rev. Sci. Eng. 40 (1998) 81.
[14] M. Arai, K. Usui, Y. Nishiyama, J. Chem. Soc., Chem. Commun. 24 (1993) 1853.
[15] M. Arai, A. Obata, K. Usui, M. Shirai, Y. Nishiyama, Appl. Catal. A: Gen. 146 (1996) 381.
[16] Y. Li, Z.-G. Li, R.-X. Zhou, J. Mol. Catal. A: Chem. 279 (2008) 140.
[17] D.G. Blackmond, T. Oukaci, B. Blanc, P. Gallezot, J. Catal. 131 (1991) 401.
[18] M.A. Vannice, B. Sen, J. Catal. 115 (1989) 65.
[19] F. Coloma, A. Sepúlveda-Escribano, F. Rodríguez-Reinoso, Appl. Catal. A: Gen. 123 (1995) L1.
[20] F. Coloma, A. Sepúlveda-Escribano, J.L.G. Fierro, F. Rodríguez-Reinoso, Appl. Catal. A: Gen. 150 (1997) 165.
[21] A.B. da Silva, E. Jordão, M.J. Mendes, P. Fouilloux, Appl. Catal. A: Gen. 148 (1997) 253.
[22] T. Ekou, A. Vicente, G. Lafaye, C. Especel, P. Marecot, Appl. Catal. A: Gen. 314 (2006) 73.
[23] M. Englisch, V.S. Ranade, J.A. Lercher, J. Mol. Catal. A: Chem. 121 (1997) 69.
[24] P. Fouilloux, in: M. Guisnet, J. Barrault, C. Bouchoule, D. Duprez, C. Montassier, G. Pérot (Eds.),Heterogeneous Catalysis in Fine Chemicals, Proc. Int. Symp., Poitiers, March 15–17, 1988, Stud. Surf. Sci. Catal., Elsevier, Amsterdam 41 (1988) 123.
[25] W. Yu, Y. Wang, H. Liu, W. Zheng, J. Mol. Catal. A: Chem. 112 (1996) 105.
[26] F. Coloma, A. Sepúlveda-Escribano, J.L.G. Fierro, F. Rodríguez-Reinoso, Appl. Catal. A: Gen. 148 (1996) 63.
[27] S. Galvagno, A. Donato, G. Neri, R. Pietropaolo, G. Capannelli, J. Mol. Catal. 78 (1993) 227.
[28] G. Neri, L. Mercadante, C. Milone, R. Pietropaolo, S. Galvagno, J. Mol. Catal. A: Chem. 108 (1996) 41.
[29] C. Neri, C. Milone, A. Donato, L. Mercadante, A.M. Visco, J. Chem. Technol. Biotechnol. 60 (1994) 83.
[30] W. Yu, H. Liu, M. Liu, Q. Tao, J. Mol. Catal. A. Chem. 138 (1999) 273.
[31] M. del Aguirre, P. Reyes, M. Oportus, I. Melián-Cabrera, J.L.G. Fierro, Appl. Catal. A: Gen. 233 (2002) 183.
[32] I.M. Vilella, I. Borbáth, J.L. Margitfalvi, K. Lázár, S.R. de Miguel, O.A. Scelza, Appl. Catal. A: Gen. 326 (2007) 37.
[33] A. Borgna, B.G. Anderson, A.M. Said, H. Bluhm, M. Hävecker, A. Knop-Gericke, A.E.T. (Ton) Kuiper, Y. de Tamminga, J.W. (hans) Niemantsverdriet, J. Phys. Chem. B 108 (2004) 17905.
[34] F. Delbecq, P. Sautet, J. Catal. 152 (1995) 217.
[35] F.W. Lytle, R.B. Greegor, E.B. Marques, D.R. Sandstroem, G.H. Via, J.H. Sinfelt, J. Catal. 95 (1985) 546.
[36] B. Moraweck, G. Clugnet, A. Renouprez, Surf. Sci. 106 (1981) 35.
[37] A.J. Marchi, D.A. Gordo, A.F. Trasarti, C.R. Apesteguía, Appl. Catal. A: Gen. 249 (2003) 53.
[38] E.C. Marques, D.R. Sandstroem, F.W. Lytle, R.B.J. Greegor, J. Phys. Chem. 77 (1982) 1027.
[39] F.W. Lytle, P.S.P. Wei, R.B. Gregor, G.H. Via, J.H. Sinfelt, J. Chem. Phys. 70 (1979) 4849.
[40] J. Stöhr, J. Electron. Spectrosc. Relat. Phenom. 75 (1999) 253.
[41] A. Borgna, T.F. Garetto, C.R. Apesteguía, B. Moraweck, Appl. Catal. A: Gen. 182 (1999) 189.
[42] A. Borgna, S.M. Stagg, D. Resasco, J. Phys. Chem. 102 (26) (1998) 5077.
[43] B. Moraweck, A.J. Renouprez, E.K. Hill, R. Baudoing-Savois, J. Phys. Chem. 97 (1993) 4288.
[44] B. Moraweck, P. Bondot, D. Goupil, P. Fouilloux, A.J. Renouprez, J. Phys. (Paris) 47 (C8) (1986) 279.
[45] E.L. Rodrigues, A.J. Marchi, C.R. Apesteguia, J.M.C. Bueno, Appl. Catal. A: Gen. 294 (2005) 197.